

Cite this: *Chem. Commun.*, 2011, **47**, 4102–4104

www.rsc.org/chemcomm

COMMUNICATION

Sodium magnesium amidoborane: the first mixed-metal amidoborane†

Hui Wu,^{*ab} Wei Zhou,^{ab} Frederick E. Pinkerton,^c Martin S. Meyer,^c Qingrong Yao,^{ad} Srinivas Gadipelli,^{ae} Terrence J. Udovic,^a Taner Yildirim^{ae} and John J. Rush^{ab}

Received 27th December 2010, Accepted 3rd February 2011

DOI: 10.1039/c0cc05814a

The first example of a mixed-metal amidoborane $\text{Na}_2\text{Mg}(\text{NH}_2\text{BH}_3)_4$ has been successfully synthesized. It forms an ordered arrangement in cation coordinations, *i.e.*, Mg^{2+} bonds solely to N^- and Na^+ coordinates only with BH_3 . Compared to ammonia borane and monometallic amidoboranes, $\text{Na}_2\text{Mg}(\text{NH}_2\text{BH}_3)_4$ can release 8.4 wt% pure hydrogen with significantly less toxic gases.

Suitable hydrogen storage materials are urgently needed for hydrogen fuel cell vehicle applications. Such compounds with a high hydrogen content and superior properties are essential for hydrogen-based energy development. Metal amidoboranes $\text{M}(\text{NH}_2\text{BH}_3)_x$ (or MAB) with the rarely seen NH_2BH_3^- anion group have been recently recognized and their potential as hydrogen storage materials widely explored.^{1–8} These compounds are found to exhibit collective advantageous properties over ammonia borane (NH_3BH_3 , AB) in terms of reduced dehydrogenation temperatures, accelerated H_2 release kinetics, and minimized borazine release. In addition, the NH_2BH_3^- group and its related ligands $(\text{R})\text{NH}-\text{BH}_2(\text{R}')^-$ are found as key components in many organometallic compounds.^{9–12} The structures and properties of these derivatives are relevant to the thriving field of catalytic hydrogen generation from AB,^{13,14} and to the mechanism of the early stages of dehydrogenation of metal amidoboranes.⁹ More recently, the NH_2BH_3^- group was also reported as an important substitute for the ethyl anion CH_2CH_3^- to enhance the agostic interaction between the metal center and the C–H bond to form more stable organometallic complexes.¹⁵

However, due to the limited number of metal amidoboranes reported so far (*i.e.* LiNH_2BH_3 ,^{1–3} NaNH_2BH_3 ,^{1,8} KNH_2BH_3 ,⁶ $\text{Ca}(\text{NH}_2\text{BH}_3)_2$,^{3,4} and $\text{Sr}(\text{NH}_2\text{BH}_3)_2$),⁷ many

possibly interesting properties of this class of compounds have yet to be recognized, and the information on the nature of NH_2BH_3^- and related ligands is thus far inadequate. Regarding hydrogen storage applications, despite the better dehydrogenation properties of MABs with respect to AB, the purity of hydrogen released was later found to suffer from the simultaneous formation of ammonia for almost all MAB compounds.^{7,16,17} The recently discovered KNH_2BH_3 was claimed to be free of ammonia,⁶ but the heavy potassium metal compromises the goal of high-hydrogen capacity. Therefore, it would be of great interest to discover and develop new $\text{MM}'(\text{NH}_2\text{BH}_3)_x$ complexes containing cheap, abundant, light-weight metals. Fabricating new amidoborane complexes with mixed cations offers a novel route to tune the thermodynamics of high hydrogen content materials. Previous studies³ suggested that the improved dehydrogenation properties of amidoborane are likely related to changes in the bonding nature of NH_2BH_3^- when it interacts with metal cations. Recent experimental and computational studies suggested a strong dependence of dehydrogenation rate on the ionicity and size of metal species in MABs.^{18,19} Therefore, introducing multiple metal species with various sizes, charges, electro-negativities, and coordination preferences could increase the array of possible bonding interactions with the NH_2BH_3^- group, ultimately allowing one to tailor more favorable modified materials properties compared to monometallic amidoboranes.

Herein, we report the synthesis, crystal structure, and dehydrogenation properties of the first example of a mixed alkali and alkaline earth metal amidoborane, $\text{Na}_2\text{Mg}(\text{NH}_2\text{BH}_3)_4$. Unlike the monometallic amidoboranes, where the cation interacts with both N^- and BH_3 units, in $\text{Na}_2\text{Mg}(\text{NH}_2\text{BH}_3)_4$, each cation coordinates solely with one type of end unit in the NH_2BH_3^- group through either ionic bonding or weak electrostatic/van der Waals interactions. Such a structure with distinct cation–anion bonding environment ordering is found to have a great impact on the dehydrogenation properties. As a result, $\text{Na}_2\text{Mg}(\text{NH}_2\text{BH}_3)_4$ can release 8.4 wt% pure hydrogen starting at 65 °C with little contamination from toxic gases such as borazine, ammonia, or diborane.

X-Ray diffraction data were collected on samples prepared by direct ball milling of varying initial ratios of $\text{NaH}:\text{MgH}_2:\text{AB}$ powders. A mixed-metal amidoborane compound with a stoichiometry of $\text{Na}_2\text{Mg}(\text{NH}_2\text{BH}_3)_4$ was identified from the data as having the space group $I4_1/a$ and approximate lattice

^a NIST Center for Neutron Research, National Institute of Standards and Technology, Gaithersburg, MD 20899-6102, USA.

E-mail: huifu@nist.gov

^b Department of Materials Science and Engineering, University of Maryland, College Park, MD 20742-2115, USA

^c Sciences and Materials Systems Laboratory, General Motors Research and Development Center, Warren, MI 48090-9055, USA

^d Guilin Electronic University, Guilin, China

^e Department of Materials Science and Engineering, University of Pennsylvania, Philadelphia, PA 19104-6272, USA

† Electronic supplementary information (ESI) available: Experimental section; crystallographic data of $\text{Na}_2\text{Mg}(\text{NH}_2\text{BH}_3)_4$; XRD pattern; neutron vibrational spectra; volumetric temperature programmed desorption results. CCDC 809738. For ESI and crystallographic data in CIF or other electronic format see DOI: 10.1039/c0cc05814a

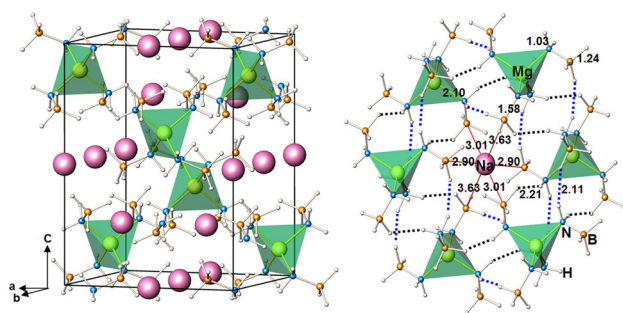


Fig. 1 Crystal structure and bonding environments of $\text{Na}_2\text{Mg}(\text{NH}_2\text{BH}_3)_4$. Each Mg^{2+} is bonded to N[−] of four NH_2BH_3^- groups, forming a $\text{Mg}(\text{NH}_2\text{BH}_3)_4$ tetrahedron, and each Na^+ is octahedrally coordinated to the BH_3 units of six NH_2BH_3^- groups. Na, pink; Mg, yellow; N, blue; B, orange; H, white. Distances are measured in angstroms.

parameters $a = 9.415 \text{ \AA}$ and $c = 12.413 \text{ \AA}$. The structure was solved using the direct space method. Detailed crystallographic data are listed in Table S1 (ESI†) and the Rietveld fit to the diffraction pattern is shown in Fig. S1 (ESI†). Note that the refinement based on laboratory X-ray data cannot provide highly accurate atomic coordinates, especially for H. First-principles calculations were thus performed to optimize the atomic positions, and the fully relaxed structure is used in the bond length discussion below. The structure of $\text{Na}_2\text{Mg}(\text{NH}_2\text{BH}_3)_4$ is illustrated in Fig. 1. The divalent Mg^{2+} connects exclusively with four NH_2BH_3^- units via Mg–N ionic bonds, forming a $\text{Mg}[\text{NH}_2\text{BH}_3]_4$ tetrahedron. The Mg–N distance is 2.104 \AA (four Mg–N), similar to the Mg–N bond lengths in $\text{Mg}(\text{NH}_2)_2$ ($1.997\text{--}2.172 \text{ \AA}$).²⁰ The monovalent Na^+ octahedrally coordinates only with six BH_3 units with Na–B separations in the range of $2.900\text{--}3.634 \text{ \AA}$, similar to Na–B distances in NaBH_4 (3.065 \AA),²¹ resulting in a distorted octahedral environment. The distances between Na and nearby hydridic H in BH_3 units range from 2.383 to 2.943 \AA . As a result, Na^+ and Mg^{2+} are tied through different interactions with two different end units of the bridging NH_2BH_3^- groups (Fig. 1), and form an ordered structure in coordinations. The particular ion coordination (*i.e.*, Mg with N and Na with BH_3) is possibly the result of accommodation of different cation sizes, charges and coordination preferences. The charge of small size Mg^{2+} (similar to monovalent Li^+ , $r_{\text{Mg}^{2+}} + (\text{VI}) = 0.57 \text{ \AA}$, $r_{\text{Li}^+ + (\text{VI})} = 0.59 \text{ \AA}$) cannot be fully compensated by the relatively large NH_2BH_3^- groups by bonding to both N and BH_3 in a tetrahedral coordination as found in LiNH_2BH_3 .³ This is further evidenced by the instability of $\text{Mg}(\text{NH}_2\text{BH}_3)_2$.²² One way to maximize the charge compensation and satisfy the tetrahedral coordination of Mg is to solely bond to N[−] of the NH_2BH_3^- groups. As a compromise, Na^+ coordinates only with BH_3 on the other end of the NH_2BH_3^- groups.

In the $\text{Na}_2\text{Mg}(\text{NH}_2\text{BH}_3)_4$ structure, the B–N bond length (1.57 \AA) is slightly shorter than in AB (1.59 \AA). The DFT calculated N–H bond lengths (1.028 \AA) are similar to the N–H in AB (1.030 \AA), while the B–H bond lengths (1.238 \AA) are much longer than those in AB (1.224 \AA). All these changes in NH_3BH_3 after it is deprotonated are consistent with those observed in the MABs (see Table S2, ESI†), suggesting a

significant change in the nature of the hydridic H on B compared to pure AB. The structure and the bonding environment of $\text{Na}_2\text{Mg}(\text{NH}_2\text{BH}_3)_4$ are further investigated and supported by neutron vibrational spectroscopy (see Fig. S2, ESI†).

Another manifest distinction compared to the monometallic amidoboranes is that the shortest $\text{BH}^{\delta-} \cdots \delta^+ \text{HN}$ distance between the neighboring NH_2BH_3^- 's in $\text{Na}_2\text{Mg}(\text{NH}_2\text{BH}_3)_4$ is 2.107 \AA , slightly longer than that in AB (2.02 \AA), but much shorter than those observed in the monometallic amidoboranes, *i.e.*, LiNH_2BH_3 (2.249 \AA),³ NaNH_2BH_3 (2.717 \AA),⁶ KNH_2BH_3 (2.265 \AA),⁶ and $\text{Ca}(\text{NH}_2\text{BH}_3)_2$ (2.328 \AA).³ Therefore, the NH_2BH_3^- units can establish a strong intermolecular dihydrogen bonding network, which together with the cation–anion interactions is responsible for the stabilization of the structure of $\text{Na}_2\text{Mg}(\text{NH}_2\text{BH}_3)_4$.

Fig. S4 (ESI†) and Fig. 2 show the thermal decomposition of $\text{Na}_2\text{Mg}(\text{NH}_2\text{BH}_3)_4$ obtained using volumetric temperature programmed desorption (TPD) analysis and independent thermogravimetry with mass spectroscopy (TGA-MS). $\text{Na}_2\text{Mg}(\text{NH}_2\text{BH}_3)_4$ started to release hydrogen at as low as 65°C for a total of 8.4 wt\% hydrogen released below 200°C with a residual product of $\text{Na}_2\text{Mg}(\text{NBH}_4)$. The TGA spectra were dominated by H_2 . The second and third peaks were quite

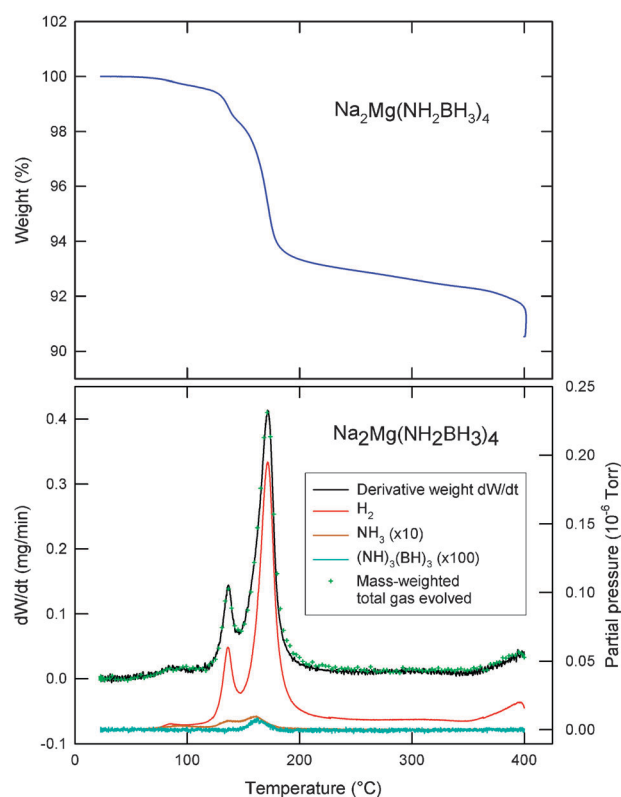


Fig. 2 TGA weight loss (upper panel) and the accompanying MS partial pressures (lower panel) for $\text{Na}_2\text{Mg}(\text{NH}_2\text{BH}_3)_4$ measured at $1.7^\circ\text{C min}^{-1}$ to 400°C . The rate of weight loss dW/dt (black curve) is also shown. Note that the NH_3 signal has been multiplied by a factor of 10 and the $(\text{NH}_3)_3(\text{BH}_3)_3$ signal has been multiplied by 100 to be visible on the same scale as H_2 . The green crosses are the total mass contribution $\text{H}_2 + \text{NH}_3 + \text{borazine}$ to the evolved gas, scaled to compare with dW/dt .

reproducible in TGA from sample to sample. In contrast, the lowest temperature peak varied in size from sample to sample, strongly suggesting that it is not intrinsic to the $\text{Na}_2\text{Mg}(\text{NH}_2\text{BH}_3)_4$ compound. It likely originates from decomposition of or reaction with other impurities in the sample, such as the unreacted NH_3BH_3 . Excluding the first peak, the observed ammonia amounts to <1 mol% of the evolved gas, and the trace of borazine in the leading edge of the third peak totals ~ 200 ppm. The ammonia is significantly suppressed compared to the monometallic amidoboranes prepared by the same ball milling method,^{6,7,16,17} e.g. ~ 15.4 mol% NH_3 was observed in NaNH_2BH_3 . The ammonia detected (as well as the trace borazine) may also be from a small amount of unreacted AB left during the synthesis as suggested recently.¹⁸ The XRD after hydrogen release is dominated by an amorphous product with a minor NaBH_4 phase (Fig. S5, ESI†). The amidoborane cannot be regenerated by direct pressurizing under 83 bar of hydrogen. Possible chemical regeneration needs further investigation.

Compared to almost all monometallic amidoboranes, $\text{Na}_2\text{Mg}(\text{NH}_2\text{BH}_3)_4$ shows significantly reduced ammonia release. The mechanism that leads to substantial NH_3 formation during the thermolysis of monometallic amidoboranes is not fully known. Based on the NMR and IR observations on the decomposition of NaNH_2BH_3 , Grochala and Fijalkowski proposed a mechanism on NH_3 emission, which involves a head-to-tail dimerization and the formation of an intermediate $\text{Na}^+[\text{BH}_3(\text{NH}_2)\text{BH}_3]^-$ salt.¹⁷ Such dimerization has also been suggested as one important path in AB^{23} and calcium amidoborane.²⁴ An N–B chain oligomerization pathway in the alkali metal amidoboranes was also found in a recent theoretical study.¹⁹ The minimization of NH_3 in $\text{Na}_2\text{Mg}(\text{NH}_2\text{BH}_3)_4$ is likely related to its unique structure motif and the ionic character of the cations, which favors the H_2 release. According to the previous proposed dehydrogenation mechanism of MAB, an intermediate M–H cluster would form involving the M–N bond and B–H bond breaking.^{25,26} Such an intermediate M–H cluster was believed to play a catalytic role in the hydrogen release process of MAB. In $\text{Na}_2\text{Mg}(\text{NH}_2\text{BH}_3)_4$, Na^+ cations do not bond to N^- but only to BH_3 units. Therefore, the intermediate catalytic NaH can form without any M–N bond breaking. In addition, another recent calculation predicted that of all alkali and alkaline earth metal amidoboranes, NaNH_2BH_3 shows the most accelerated hydrogen release rate.¹⁹ It also suggested that magnesium amidoborane would release hydrogen via a “direct” pathway instead of by an N–B chain oligomerization pathway. The latter was found in the MAB systems with significant NH_3 detected as mentioned above.¹⁷ Therefore, the co-existing Na^+ and Mg^{2+} cations accentuate the H_2 release, which will surpass the formation and release rate of NH_3 . As a result, the gas released from $\text{Na}_2\text{Mg}(\text{NH}_2\text{BH}_3)_4$ is predominantly H_2 .

In summary, the first example of a mixed-metal amidoborane, $\text{Na}_2\text{Mg}(\text{NH}_2\text{BH}_3)_4$, was synthesized through the direct ball milling of hydrides and ammonia borane. The crystal structure was determined via X-ray powder diffraction and first-principles calculations. $\text{Na}_2\text{Mg}(\text{NH}_2\text{BH}_3)_4$ releases 8.4 wt%

pure hydrogen with minimal ammonia and borazine contamination, and no detectable diborane. Our study demonstrates that hydrogen release properties of amidoboranes can be rationally and significantly improved by tuning the atomic interactions and thus producing more desired structures through the formation of mixed-metal amidoboranes.

This work was partially supported by DOE through BES Grant No. DE-FG02-08ER46522 (G.S. and T. Y.) and EERE Grant No. DE-AI-01-05EE11104 (T. J. U.).

Notes and references

- Z. Xiong, C. K. Yong, G. Wu, P. Chen, W. Shaw, A. Karkamkar, T. Autrey, M. O. Jones, S. R. Johnson, P. P. Edwards and W. I. F. David, *Nat. Mater.*, 2007, **7**, 138–141.
- X. Kang, Z. Fang, L. Kong, H. Cheng, X. Yao, G. Lu and P. Wang, *Adv. Mater.*, 2008, **20**, 2756–2759.
- H. Wu, W. Zhou and T. Yildirim, *J. Am. Chem. Soc.*, 2008, **130**, 14834–14839.
- H. V. K. Diyabalanage, R. P. Shrestha, T. A. Semelsberger, B. L. Scott, M. E. Bowden, B. L. Davis and A. K. Burrell, *Angew. Chem., Int. Ed.*, 2007, **46**, 8995–8997.
- C. Wu, G. Wu, Z. Xiong, X. Han, H. Chu, T. He and P. Chen, *Chem. Mater.*, 2010, **22**, 3–5.
- H. V. K. Diyabalanage, T. Nakagawa, R. P. Shrestha, T. A. Semelsberger, B. L. Davis, B. L. Scott, A. K. Burrell, W. I. F. David, K. R. Ryan, M. O. Jones and P. P. Edwards, *J. Am. Chem. Soc.*, 2010, **132**, 11836–11837.
- Q. Zhang, C. Tang, C. Fang, F. Fang, D. Sun, L. Ouyang and M. Zhu, *J. Phys. Chem. C*, 2010, **114**, 1709–1714.
- Z. Xiong, Y. S. Chua, G. Wu, W. Xu, P. Chen, W. Shaw, A. Karkamkar, J. Linehan, T. Smurthwaite and T. Autrey, *Chem. Commun.*, 2008, 5595–5597.
- J. Spielmann, G. Jansen, H. Bandmann and S. Harder, *Angew. Chem., Int. Ed.*, 2008, **47**, 6290–6295.
- A. C. Hillier, T. Fox, H. W. Schmalke and H. J. Berke, *J. Organomet. Chem.*, 2003, **669**, 14–24.
- P. Binger, F. Sandmeyer and C. Krger, *Organometallics*, 1995, **14**, 2969–2976.
- M. D. Fryzuk, B. A. MacKay, S. A. Johnson and B. O. Patrick, *Angew. Chem., Int. Ed.*, 2002, **41**, 3709–3712.
- J. Spielmann and S. Harder, *J. Am. Chem. Soc.*, 2009, **131**, 5064–5065.
- P. M. Zimmerman, A. Paul, Z. Zhang and C. B. Musgrave, *Angew. Chem., Int. Ed.*, 2009, **48**, 2201–2205.
- T. D. Forster, H. M. Tuononen, M. Parvez and R. Roesler, *J. Am. Chem. Soc.*, 2009, **131**, 6689–6691.
- T. Autrey, PNNL Progress as Part of the Chemical Hydrogen Storage Center of Excellence, DOE Hydrogen Annual Merit Review 2009 (http://www.hydrogen.energy.gov/pdfs/review09/st_18_autrey.pdf).
- K. J. Fijalkowski and W. Grochala, *J. Mater. Chem.*, 2009, **19**, 2043–2050.
- A. T. Luedtke and T. Autrey, *Inorg. Chem.*, 2010, **49**, 3905–3910.
- D. Y. Kim, H. M. Lee, J. Seo, S. K. Shin and K. S. Kim, *Phys. Chem. Chem. Phys.*, 2010, **12**, 5446–5453.
- M. H. Sorby, Y. Nakamura, H. W. Brinks, T. Ichikawa, S. Hino, H. Fujii and B. C. Hauback, *J. Alloys Compd.*, 2007, **428**, 297–301.
- Y. Filinchuk and H. Hagemann, *Eur. J. Inorg. Chem.*, 2008, 3127–3133.
- Y. S. Chua, G. Wu, Z. Xiong, A. Karkamkar, J. Guo, M. Jian, M. W. Wong, T. Autrey and P. Chen, *Chem. Commun.*, 2010, **46**, 5752.
- A. C. Stowe, W. J. Shaw, J. C. Linehan, B. Schmi and T. Autrey, *Phys. Chem. Chem. Phys.*, 2007, **9**, 1831.
- J. Spielmann, G. Jansen, H. Bandmann and S. Harder, *Angew. Chem., Int. Ed.*, 2008, **47**, 1.
- D. Y. Kim, S. K. Shin, H. M. Lee and K. S. Kim, *Chem.–Eur. J.*, 2009, **15**, 5598.
- T. B. Lee and M. L. McKee, *Inorg. Chem.*, 2009, **48**, 7564.